Taylor & Francis
Taylor & Francis Group

SEPARATION SCIENCE AND TECHNOLOGY

Separation Science and Technology

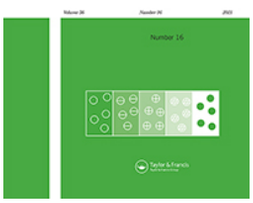

ISSN: (Print) (Online) Journal homepage: https://www.tandfonline.com/loi/lsst20

Capacity of ethanol adjunct-treated interface of ionic liquid aqueous two phase system in simultaneous extraction and purification of sorghum leaf sheath polysaccharides

Otu Phyllis Naa Yarley, Azumah Bright Kojo, Ahmed Mohammed Gedel, Cunshan Zhou, Xiaojie Yu, Osae Richard, Tetteh Ebenezer Ababio, Haonan Jiang & Hongpeng Yang

To cite this article: Otu Phyllis Naa Yarley, Azumah Bright Kojo, Ahmed Mohammed Gedel, Cunshan Zhou, Xiaojie Yu, Osae Richard, Tetteh Ebenezer Ababio, Haonan Jiang & Hongpeng Yang (2021) Capacity of ethanol adjunct-treated interface of ionic liquid aqueous two phase system in simultaneous extraction and purification of sorghum leaf sheath polysaccharides, Separation Science and Technology, 56:16, 2750-2765, DOI: 10.1080/01496395.2020.1844237

To link to this article: https://doi.org/10.1080/01496395.2020.1844237

SEPARATION SCIENCE AND TECHNOLOGY
2021, VOL. 56, NO. 16, 2750–2765
https://doi.org/10.1080/01496395.2020.1844237

Capacity of ethanol adjunct-treated interface of ionic liquid aqueous two phase system in simultaneous extraction and purification of sorghum leaf sheath polysaccharides

Otu Phyllis Naa Yarley[a,b], Azumah Bright Kojo[b], Ahmed Mohammed Gedel[b], Cunshan Zhou[a], Xiaojie Yu[a], Osae Richard[c], Tetteh Ebenezer Ababio[a], Haonan Jiang[a], and Hongpeng Yang[a]

[a]School of Food and Biological Engineering, Jiangsu University, Zhenjiang, China; [b]Faculty of Applied Sciences, Department of Science Laboratory Technology, Accra Technical University, Accra, Ghana; [c]School of Applied Science and Technology, Department of Food and Postharvest Technology, Cape Coast Technical University, PMB, Cape Coast, DL 50, Ghana

ABSTRACT

Employing response surface methodology, partially purified polysaccharides from *Sorghum bicolor* L. leaf sheath were extracted using synergized ethanol adjunct-treated ionic liquid aqueous two phase system (1-octyl-3-methylimidazolium chloride, [C_8mim]Cl and K_2CO_3) and dual frequency ultrasound-assisted extraction. Under ultrasound conditions of 35 °C, 20&60 KHz, 25 mins an experimental yield of 16% PPS was achieved. Dual frequency ultrasound-assisted dialysis effectively reduced salt content of extracted PPS solution in a liquid membrane. The polysaccharides collected after dialysis maintained primary structures. The introduction of ethanol in the ionic liquid aqueous two phase system therefore ensured an excellent simultaneous extraction and partial purification.

ARTICLE HISTORY
Received 5 September 2019
Accepted 23 October 2020

KEYWORDS
Sorghum bicolor L.; ethanol adjunct; liquid membrane dialysis; rheology; bioactivity

Introduction

Currently, scientists into bioseparation have undivided attention on efficient simultaneous separation and purification of macromolecules from natural sources using methods that are eco-friendly liquids, cut down time and cost of using traditional methods. Progressively, extraction of plant crude polysaccharides followed by purification process using ionic liquid aqueous two phase system (ILATPS) has been reported by Tan et al. (2012)[1] and in a previous work Otu et al. (2018).[2] Merging two protocols becomes advantageous to the food industry, since time and cost into crude polysaccharide extraction can be minimized. It is thus paramount to develop a high yield simultaneous process for the separation and purification of macromolecules.

Interfacial tension is known to exist between the surfaces (or interface) of two immiscible liquids. The greater the dissimilarity between the two phases, the greater the interfacial tension.[3] Meanwhile, it has been established that solvents with as low as 15 dynes/cm interfacial tension can best penetrate targeted compounds.[4] The need for a low interfacial tension can be achieved by the introduction of other solvents which usually act to reduce interfacial-free energy.[3] Hydrophilic surfaces are highly negatively charged and therefore attract positively charged solvent causing their cationic head group chains to orient toward the solution leading to electrostatic double layer repulsion and thus decrease in hydrophobic interaction and subsequent decrease in cohesion.[5] Therefore in an attempt to achieve higher extraction yield, anti-solvent was employed which is known to be a solvent in which targeted compounds are less soluble but possess hydrophilic stabilizers[6] and thus can greatly reduce interfacial tension between solvents when applied at a very low concentration. Specifically, ethanol was employed as a form of adjunct in the ionic liquid aqueous two phase system to aide in the reduction of interfacial tension at the salt-rich – ionic liquid-rich (liquid-liquid) interface and thus penetrate better the polysaccharide matrices of Sorghum leaf sheath and further increase yield of extracted polysaccharides. To the best of our knowledge the introduction of ethanol as an adjunct in an ionic liquid aqueous two phase system (EA-ILATPS) for the simultaneous separation and purification of polysaccharide in this work has not yet been reported.

Intermolecular associations of polysaccharides, degree of branching and glycosidic branching are among some chemical properties that directly affect the antioxidant properties of polysaccharides.[7–9] Therefore, obvious ways by which chemical properties of targeted compound can be interfered must be avoided by researchers. For example, the helical structure of

CONTACT Cunshan Zhou cunshanzhou@163.com School of Food and Biological Engineering, Jiangsu University, Zhenjiang 212013, China.

a template peptide has been found to be almost destroyed at a high salt concentration.[10] This implies that thorough desalination after extraction of polysaccharides by the salt-rich phase of an ILATPS can lead to the maintenance of the primary chemical structures of samples. It is also an established principle that replacement of dialyzate with fresh dialyzate will further reduce concentration of small molecules in sample. Since replacement of equilibrated dialyzate affects the diffusion of small molecules (salt) from samples, this work further varied the rate of dialyzate replacement under dual frequency ultrasound to ascertain the overall impact on the level of desalination.

Sorghum leaf sheath has high content of antioxidants, together with simple phenolic acids, as well as polyphenols, particularly 3-deoxyanthocyanidins, notably luteolinidin and apigenidin.[11,12] These phyto-constituents have been found to possess vasoprotective,[13] lipid peroxidation inhibition and free radicals scavenging characteristics.[14] The impact of extraction, purification and desalination process on the antioxidant property of purified polysaccharides (PPS) was also determined in this work.

Dual frequency type of ultrasound reactor is characterized by a strong interference pattern in the ultrasound reactor that curbs any form of directional effect. The dual frequency ultrasound provides a solution to a directional sensitivity, a shortcoming of single frequency type of ultrasound reactor that can cause varying volumetric energy dissipation in the reaction medium, thus limiting extraction yield.[15] Therefore, the objectives of this study were to:

(i) investigate the optimum volume ratio of water: ethanol for the ILATPS formation.
(ii) establish the individual and interactive effects of ultrasound-assisted process variables including dual frequency, temperature and time on the yield of partially purified polysaccharides.
(iii) optimize the operational parameters to obtain the maximum yield of pure polysaccharides using Box-Behnken Designs (BBD).
(iv) investigate the impact of dual frequency ultrasound and dialyzate replacement on the liquid membrane dialysis process.
(v) characterize the extracted purified polysaccharide and investigate the antioxidant activity in-vitro.

Materials and methods

Preparation of powder sample

Dried *S. bicolor* leaf sheath was obtained from Ghana. The leaf sheath was pulverized into powder and sieved through a 100-mesh screen. Majority of monosaccharides, pigments and fats were removed from the powder using ethanol (90% v/v) in a Soxhlet system at 70 °C for 4 h. The filtered residue was dried at 40 °C in a hot air oven to obtain the pretreated dry sample powder.

Phase diagram

The phase diagrams were determined by the cloud point titration method at atmospheric pressure and at a temperature of 298.15 K, which was maintained constant by using a water thermostat (KW-1000DC, Jintan Zhongda Instrument Factory, China). Aqueous solutions composed of 50 wt% K_2CO_3 and aqueous solutions of [$C_n$mim]Cl at 50 wt% were prepared and used for determination of the binodal curves.[16,17]

For comparison purpose, a 20%v/v ethanol-water was used to prepare ionic liquid (IL) and salt solution for the binodal control system. The concentration of ethanol was kept constant in all systems. The aqueous inorganic salt solution was added drop-wise to the IL aqueous solution until the detection of a cloudy solution (biphasic region), followed by the drop-wise addition of water until the formation of a clear solution (monophasic region). The weights of the added components were recorded. The drop-wise addition was carried out under constant shaking. The composition of each ternary system was determined by weight quantification of all components within ± 10^{-4} g (using an analytical balance, PRACTUM124-1CN from Sartorius Scientific Instruments Co., Beijing). The phase diagram experiments were repeated three times and the average weight was obtained. The binodal data of these systems were correlated using the Merchuk equation (Eq. (1)).[18]

$$Y = A\exp(BX^{0.5} - CX^3) \quad (1)$$

Where Y and X are the PEG and salt weight percentages, respectively, and A, B, and C are the fitting parameters obtained by regression of the data.

Choice of ethanol concentration in ILATPS

To three different sets of 15 ml centrifuge tubes, 35% (w/w) of [C_8 mim]Cl (1-octyl-3-methylimidazolium chloride), 17% (w/w) of K_2CO_3 and pretreated powdered sample were added. Finally, 48% (w/w) of ethanol: Water volume ratios of 20:80, 40:60, 60:40% v/v were added, respectively. The mixtures were vortex to mix well under room temperature. Purified polysaccharides were extracted into salt-rich phase using DF-UAE operational conditions (20&60 KHz, temperature 30 °C and time 30 min) of ultrasound water bath under continuous

mode (5 seconds on for each frequency). The phase separation was speeded using centrifugation at 2000 rpm for 5 min and thus two clear phases were formed. The polysaccharide content of the bottom phase was measured using the phenol-sulfuric method. The polysaccharide content was calculated using the formula in Equation (1):

$$\text{Yield}(\%) = C * V/W * 100 \quad (2)$$

Where C (g/ml) is the concentration of polysaccharide solution, V (ml) is the volume of bottom phase and W (g) is the weight of purified polysaccharide.

Preparation of EA-ILATPS and polysaccharide separation

To a 15 ml centrifuge tube, 35% (w/w) of [C_8 mim]Cl, 17% (w/w) of K_2CO_3, 48% (w/w) of ethanol: water volume ratio (40:60% v/v) (based on results obtained, Fig. 2) and pretreated powdered sample was added. Another mixture with the same phase components without crude polysaccharide was prepared as blank to avoid interference. The mixture was vortex to mix well under room temperature. Purified polysaccharides were extracted into salt-rich phase using designed dual frequency, temperature and time of an ultrasound water bath under continuous mode (5 seconds on for each frequency). Purified polysaccharide content was calculated using formula described under section 2.3.

Liquid membrane dialysis of polysaccharide

Desalination was achieved as described by Zhang et al. (2018) with brief modification.[19] Partially purified polysaccharide extracted into the salt-rich phase under optimum dual ultrasound operating parameters was dialyzed using a recyclable dialysis membrane (D44 mm, MWCO 8000–14000), enabling the filtration of the salt and IL. The dialysis membranes containing polysaccharide – salt-rich solutions (SL-D_{20}P and SL-D_{30}P) were dialyzed under ultrasound conditions (20&60 KHz, 25 °C, and 60 mins), while replacing dialyzate (water, 300 ml) every 20 mins and 30 min, respectively, within 1 h and further kept in dialyzate for 5 h without ultrasound. The extracted polysaccharides were lypholized for further characterization.

Single-factor design

As a preliminary tool, single-factor design was developed for the extraction of purified polysaccharides with extraction factors X_1 (dual frequency: 40&60, 20&40, 20&60 KHz), X_2 (extraction temperature: 25, 30, 35, 40, 45 °C) and X_3 (extraction time: 10, 20, 30, 40, 50, 60 min) each with a control group. Each experimental factor was varied as the other experimental factors were kept constant. All experiment was conducted in triplicate under a constant power of 240 W and 4 mg/ml sample concentration and the dependent variable used was the extraction yield of purified polysaccharide.

Optimization of experimental design

Three variables were selected, coded (X_1, X_2, X_3) and examined in three levels (Table 1) based on the experimental results from the single-factor experiments. A response surface methodology was then conducted using the Box-Behnken Design (BBD). It comprised of 17 experimental runs, conducted in triplicates and its experimental results has been presented (Table 2).

Preliminary characterization of polysaccharides

Total carbohydrate, proteins and polyphenolic content

The total carbohydrate and protein contents of SL-D_{20}P and SL-D_{30}P were determined according to phenol-sulfuric method[20] and Bradford Method[21] respectively. The phenolic contents were measured as described by Kumar, et al. (2008).[22]

Table 1. Variables and the corresponding three levels employed in Box-Behnken Design for simultaneously separated and purified polysaccharide extraction.

			Coded Levels		
Variable	Units	Symbol	−1	0	1
Temperature	°C	X_1	25	30	35
Dual Frequency	KHz	X_2	40&60	20&40	20&60
Time	Mins	X_3	10	20	30

Table 2. Experimental design of response surface analysis and its experimental values.

Run	X_1 Temperature (°C)	X_2 Dual frequency (KHz)	X_3 Time (mins)	Y Crude Polysaccharide (%)
1	30	20&60	30	16.32
2	25	40&60	20	9.89
3	30	20&40	20	9.42
4	25	20&60	20	9.55
5	30	20&40	20	9.27
6	35	20&40	30	7.06
7	30	20&40	20	9.42
8	25	20&40	30	3.02
9	30	20&60	10	4.13
10	35	20&60	20	16.09
11	30	40&60	30	0.90
12	35	40&60	20	9.68
13	30	20&40	20	9.50
14	25	20&40	10	2.50
15	30	40&60	10	9.60
16	30	20&40	20	7.54
17	35	20&40	10	4.70

Monosaccharide composition

Monosaccharide composition was determined using Gas chromatography (GC), a methodology described by Wang et al. (2017).[23] Briefly, 10 mg of sample was hydrolyzed in ampoules with trifluoroacetic acid (2 M, 2 ml) for 3 h at 110°C. It was then evaporated and methanol was added to remove TFA. The hydrolyzates were mixed with hydroxylamine hydrochloride (10 mg) and pyridine (0.5 ml) and allowed to incubate at 90°C for 30 min. Acetic anhydride (0.5 ml) was added and again incubated at 90°C for 30 min. The mixtures were cooled to room temperature, and then filtered using 0.22 µm filters. The resulting alditol acetates were then analyzed by GC, which was performed on a Thermo TRACE1300 instrument fitted with FID (280°C) and equipped with HP-5 column (30 m × 0.25 mm × 0.25 µm). The column temperature was maintained at 110°C for 5 min, and increased to 190°C for 4 min at a rate of 5°C/min, then increased to 210°C for 10 min at a rate of 3°C/min. Standard monosaccharide used included (D-glucose, D-xylose, D-mannose, D-galactose, D-galacturonic acid, L-arabinose). These were prepared and subjected to GC analysis separately in the same way.

Spectral analysis

Fourier transform-infrared (FT-IR)

The infrared spectra of the samples were measured between 4000 and 400 cm^{-1} absorbance mode on the FT-IR spectrophotometer (Nicolet, Nexusn670). Samples were ground with KBr (1:100 mg) and pressed into a translucent pellet. Scanning was performed with a resolution of 4 cm^{-1}.

Ultraviolet (UV) spectroscopy

The ultraviolet spectra of SL-D_{20}P and SL-D_{30} P solutions (1.0 mg/ml) were recorded with scanning UV-vis spectrophotometer (Rayleigh, UV- 1601) in the 200–400 nm region in 1.00 cm quartz cell against distilled water as blank.

Structural analysis

Tertiary structure (Congo red method)

The conformational structures of (SL-C_{20}P) and (SL-D_{30} P) were determined as described by Qui et al. (2013)[24] with little modification. Briefly, different sets of solutions were prepared containing polysaccharides (1 mg/ml, 2 ml) in (0.0–0.5 M) NaOH (increasing stepwise by 0.05 M increments using (4 M) NaOH solution) and (100 µM, 2 ml) of Congo red. These were analyzed in the range of 400–700 nm with a UV-Vis spectrophotometer and the maximum absorption wavelengths were recorded as a function of NaOH concentration. Congo red in NaOH served as the negative control.

Scanning electron microscopy (SEM)

The Scanning Electron Microscope (JSM-7001 F, JEOL, Tokyo, Japan) was used to observe the morphological characteristics of the sample polysaccharides. Each sample was coated with a conductive layer of gold-palladium.

Molecular weight (Mw)

The molecular weights (Mw) were determined by High Performance Size-Exclusion Chromatography (HPSEC) using three column; OHpak SB-806 HQ column (8.0mm ID x 300 mm), OHpak SB-805 HQ column (8.0 mm ID x 300 mm) and OHpak SB-806 HQ column (8.0 mm ID x 300 mm): Shodex®, Japan. The performance conditions were: column temperature 25°C, injection volume: 15 µl (2 mg/ml w/v) and flow rate 0.500 ml/min with KH_2PO_4 (pH 6.0), Detector: RI. Data from the light scattering instrument (HELEOS) was collected and analyzed using ASTRA 6.1.7.15 (Wyatt Technology), and the molecular weight calculated.

Particle size (Dynamic light scattering)

Hydrodynamic diameter of the purified sample in water (2 mg/ml) was determined using the dynamic light scattering methodology as described by Ren et al. (2015).[25] Briefly, the hydrodynamic diameter of the purified sample in water was examined using dynamic scattering on a Zetasizer nano ZSP (Malvern Instruments, UK). The solution containing the sample (2 mg/ml) were filtered through a (0.45µ) syringe filter. The solution was measured firstly at room temperature (25 °C) and then secondly heated at 70 °C for 1 hour 50 min (1.5 h) and then cooled down to a temperature of 25 °C and again measured. Samples were measured 10 times under each condition.

Rheological properties

The steady shear and oscillatory tests samples at a concentration of 5 mg/ml were conducted with a DHR-1 rheometer (TA Instruments, Surrey, UK) using a cone-and-plate geometry, with a cone angle of 1°, a diameter of 50 nm, and a gap of 1.0 mm. Oscillatory (dynamic) tests were performed using small deformation oscillatory rheometry at 25 °C between 10 and 0.01 Hz. The viscoelastic properties, storage modulus (G′), loss modulus (G″) and tan δ were recorded versus frequency. The steady shear measurements were performed at 25 °C between 1 and 100 s^{-1}. All measurements were done in triplicates.

Antioxidant activity in-vitro

Hydroxyl radical scavenging assay

The hydroxyl radical assay was measured using the method described by Jen et al. (1998).[26] Briefly, Samples were dissolved in distilled water (5–30 mg/ml). The sample solution (1.0 ml) was mixed with $FeSO_4$ (9 mM, 1.0 ml) and 9 mM salicylic acid solution (1 mL, 50% ethanol). Then, 8.8 mM H_2O_2 (1.0 ml) was added to start the reaction. Similarly, the background was composed of sample solution (1.0 ml) mixed with $FeSO_4$ (9 mM, 1.0 ml). In place of salicylic acid solution, 50% ethanol (1.0 ml) was used. Again, 8.8 mM H_2O_2 (1.0 ml) was added to start the reaction. For the control distilled water (1.0 ml) was substituted for the polysaccharide solution. The test sample, background group and control sample were kept in water bath at 37°C for 1 h. After warming in a water bath, the absorbance of the mixture was measured at 510 nm.

The hydroxyl radical scavenging rate was calculated using the following formula in Eq. (3):

$$\text{Scavenging Rate}(\%) = [1 - (A_1 - A_2)/A_0] \times 100\% \quad (3)$$

Where A_0 is the absorbance of the control group (without polysaccharides), A_1 is the absorbance of the test group, A_2 is the absorbance of the background group.

ABTS radical scavenging assay

The ABTS radical scavenging assay was measured using the method described by Zhou et al. (2011)[27] with slight modifications. Briefly, ABTS (50 ml, 7 mM) was mixed with 140 mM potassium peroxydisulfate (890 µl), then kept in dark at room temperature for 12–16 h before use. The samples were prepared in a variety of concentrations (5–30 mg/ml). The polysaccharide solution (0.2 mL) was added to the ABTS·+ solution (5 ml). The absorbance of the mixture was measured at 734 nm namely after holding at room temperature for 6 min. The ABTS radical scavenging rate was calculated using the following formula:

$$\text{Scavenging Rate}(\%) = [1 - (A_1 - A_2)/A_0] \times 100\% \quad (4)$$

Where A_0 is the absorbance of the control group (without polysaccharides), A_1 is the absorbance of the test group, A_2 is the absorbance of the background group (without $ABTS^+$).

Results and discussion

Choice of ionic liquid

By increasing alkyl chain length, phase forming ability with K_2CO_3 salt was found to be in the order: $[C_{10}mim]Cl \approx [C_6mim]Cl > [C_4mim]Cl > [C_8mim]Cl$. The alkyl length, $[C_8mim]Cl$ demonstrated the least phase forming ability (Fig. 1). A similar pattern was confirmed by Pei and Coworkers (2007).[28] In their report, $[C_6mim]Br > [C_8mim]Br$ in phase forming ability with K_2HPO_4 salt. The cation, $[C_6mim]^+$ was found to be the best in phase formation. The alkyl length $[C_{12}mim]Cl$ however formed the easiest immiscibility using lower concentration of salt.

The use of ethanol in solution preparation changed the observed phenomenon in phase forming abilities (Fig. 1). By increasing alkyl chain length, phase forming ability was found to be in the order: $[C_8mim]Cl > [C_{10}mim]Cl \approx [C_6mim]Cl > [C_4mim]Cl$. The remarkable improvement in phase formation of $[C_8mim]Cl$ with K_2CO_3 salt solution can be attributed to solvatrophobic interaction between the hydrocarbon portion of the ethanol and IL. The interaction guides ethanol micelles formation which tends to enhance solvation characteristics of the IL/ ethanol system.[29] Therefore, the IL $[C_8mim]Cl$ assisted with ethanol was the selected system used for this work.

Choice of ethanol concentration in ILATPS

The variation of ethanol-water solution concentrations used in the preparation of different ternary systems showed clear impact on amount of polysaccharides extracted into the bottom salt-rich phase of ATPS. Highest polysaccharides and proteins extraction efficiencies of 15.91% and 0.92% were recorded, respectively, for ternary systems prepared using 40%v/v ethanol-water solution. Further increase in concentration of ethanol-water solution-reduced polysaccharides and increased proteins extraction efficiencies in ILATPS. At a low ethanol concentration, more hydronium ion (H_3O^+) is known to be produced. This occurrence can be attributed to greater water content.[30] The pH value of low ethanol concentration becomes lower, promoting depolymerization of cellulose.[31]

Single-factor experiments

Effect of ultrasound temperature

The ultrasound temperature of 35 °C showed the highest significantly different ($p < 0.05$) yield in extracted purified polysaccharide under fixed conditions (ultrasound dual frequency: 20&40 KHz and ultrasound time: 30 mins) (Fig. 3(a)). Beyond the temperature of 35 °C, a significantly different ($p < 0.05$) reduction in polysaccharide yield was recorded for purified polysaccharide in the salt-rich phase of ionic liquid aqueous two phase system. Above a temperature 35 °C there was reduction of the salting out effect of salt since water moves from the top to the bottom, an observation confirmed by Xie et al. and Otu et al.[2,32] which leads to reduction in the amount of polysaccharides extracted. Thus, 35 °C temperatures was used for this work.

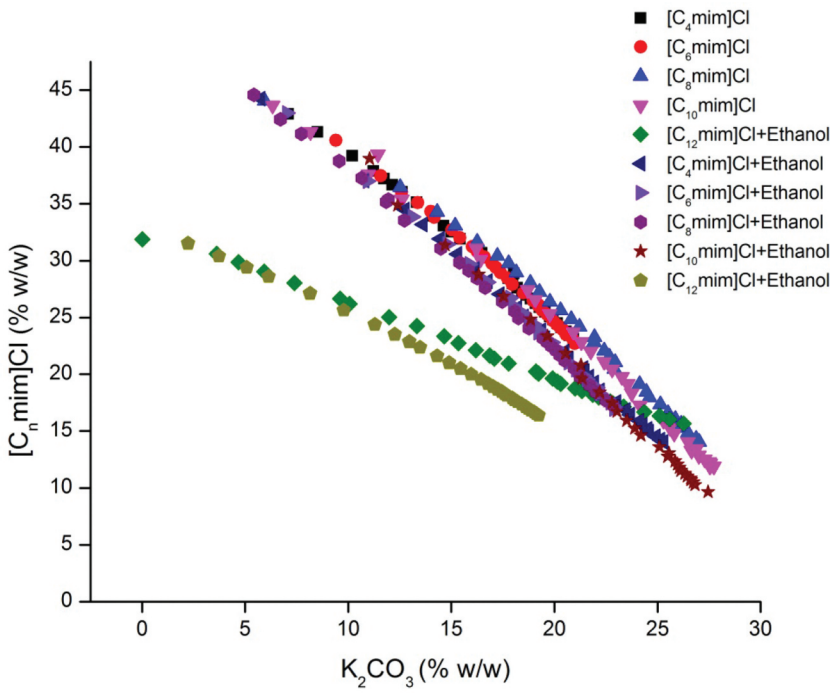

Figure 1. Phase diagrams of [$C_n$mim]Cl with and without ethanol.

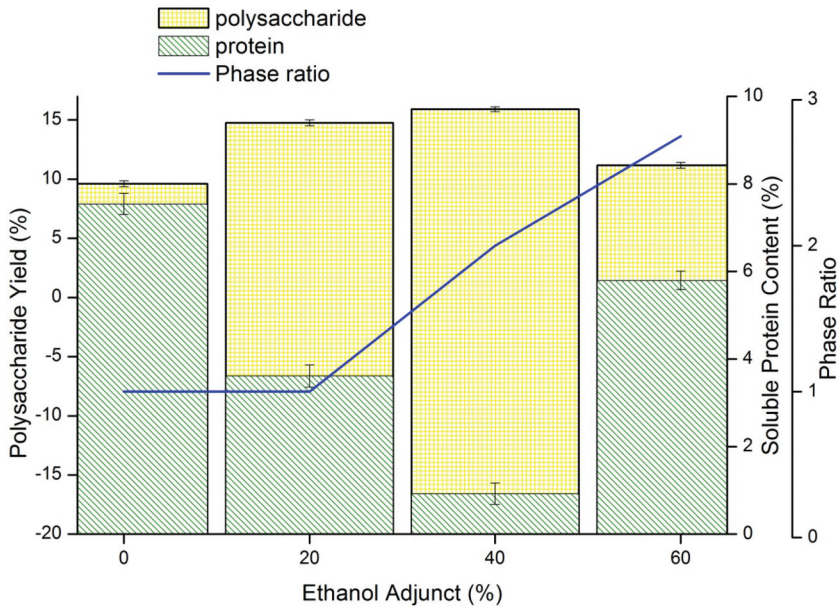

Figure 2. Effect of ethanol adjunct on the simultaneously extracted and purified polysaccharides yield in an ionic liquid aqueous two phase system, [C_8mim]Cl/K_2CO_3 under dual frequency ultrasound.

Effect of ultrasound dual frequency

The yield of simultaneously separated and purified polysaccharides based on the effect of ultrasound operational parameter, dual frequency under fixed conditions (ultrasound temperature: 30 °C and ultrasound time: 30 mins) has been shown in (Fig. 3(b)). Application of dual frequency, 20&60 KHz demonstrated the highest significantly different ($p < 0.05$) yield of pure polysaccharides. Specific ultrasound frequency difference has been found to impact higher extraction yield,[33] consistent with the observed extraction ability of ultrasound frequency 20&60 KHz.

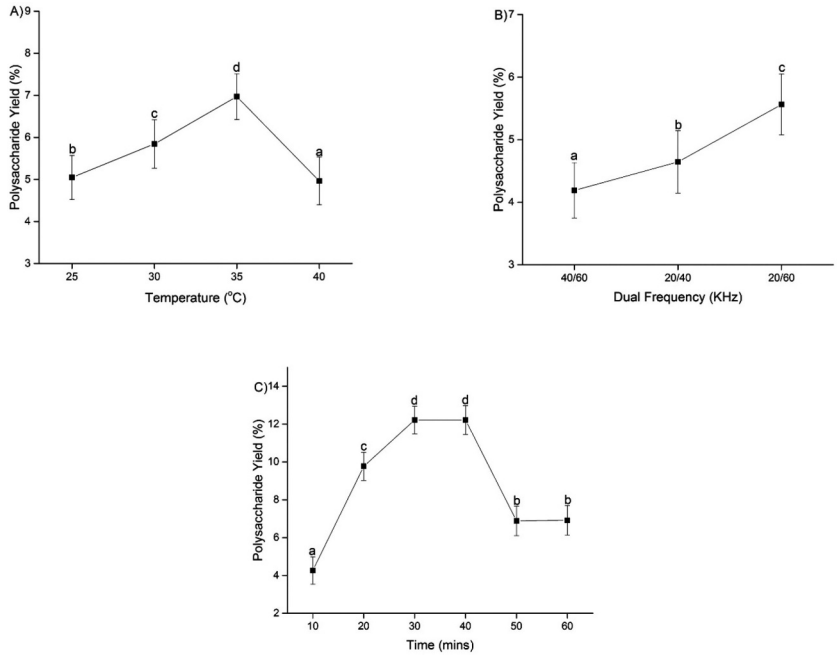

Figure 3. Effect of **A)** ultrasound temperature (25°C – 45°C) **B)** ultrasound dual frequency (40&60, 20&40, 40&60) and C) time (10–60 min) on the yield of *Sorghum* Leaf sheath extracted and partially purified polysaccharides.

Effect of ultrasound time

Under fixed conditions (ultrasound dual frequency: 20&40 KHz and ultrasound temperature: 30 °C), ultrasound time (30 mins) recorded the highest significantly different ($p < 0.05$) yield in purified polysaccharide (Fig. 3(c)). There was however no significant difference ($p < .05$) between ultrasound time, 30 min and 40 mins, making 30 mins the peak time for extraction. Increasing the time above 30 mins may have increased temperature for hydrolysis of polysaccharides to take place.[34]

Optimization using Box-Behnken design

Fitting the model

To evaluate the quality of the fitted model, analysis of variance (ANOVA) was performed (Table 3). In the model, the second-order polynomial model for the extraction of purified polysaccharide was statistically significant with a small model (< 0.0001) and satisfactory coefficient of determination (R^2 = 0.9834). The linear parameters for the purified polysaccharides were found to be at significant levels (X_1, X_2, X_3: 0.0010, 0.0002, 0.0292, respectively). Quadratic parameter (X_2^2 ,X_3^2) were found to be at significant levels (0.0002, < 0.0001, respectively) for extracted purified polysaccharide. On the other hand, interaction parameters (X_1X_2, X_2 X_3: 0.0046, < 0.0001, respectively) were at significant levels for the purified polysaccharides. The "lack of Fit-Value" of the model was not significant with a *p*-value of 0.5107. The significant regression and non-significant lack of fit indicated that the regression equation is adequate to represent the actual relationship between the response values (Y) and three independent variables of the purified polysaccharides. The quadratic regression equations obtained for the purified polysaccharide Eq. (5) is as follows:

$$Y = 9.03 + 1.57X_1 + 2.00X_2 + 0.80X_3 + 1.69X_1X_2 + 0.46X_1X_3 + 5.22X_2X_3 - 0.57X_1^2 + 2.85X_2^2 - 4.14X_3^2 \quad (5)$$

Table 3. ANOVA for Response Surface Quadratic Model for simultaneously separated and purified polysaccharide extraction.

Source	Sum of Squares	df	Mean Square	F Value	P-value Prob>F
Model	281.20	9	31.24	46.16	< 0.0001
X_1	19.72	1	19.72	29.13	0.0010
X_2	32.05	1	32.05	47.35	0.0002
X_3	5.06	1	5.06	7.47	0.0292
X_1X_2	11.36	1	11.36	16.78	0.0046
X_1X_3	0.85	1	0.85	1.25	0.2999
X_2X_3	109.14	1	109.14	161.24	< 0.0001
X_1^2	1.39	1	1.39	2.05	0.1952
X_2^2	34.10	1	34.10	50.38	0.0002
X_3^2	72.11	1	72.11	106.54	< 0.0001
Residual	4.74	7	0.68		
Lack of Fit	1.923	0.64	0.91	0.5107	
Pure Error	2.81	4	0.70		
Cor Total	285.94	16			
R-Squared	0.9834				
Adj	R Squared		0.9621		

Analysis of response surfaces

Ultrasound operation temperature when increased to about (30 °C) together with a shift toward the dual frequency of 20 & 60 KHz caused an increase in polysaccharide yield. Not much increase was observed with temperatures above (30 °C) (Fig. 4(a)). The ultrasound temperatures when increased from 25 °C to 35 °C along with increasing time from 10 mins to 25 mins also recorded an increase in polysaccharide yield. After 25 mins polysaccharide yield assumed a constant level (Fig. 4(b)). At dual frequency (20&60 KHz) the yield of polysaccharide increased from 10 mins to 25 mins (Fig. 4(c)). The combination of the analysis of variance (ANOVA) (Table 3) and response surfaces (Fig. 4) indicated that the interaction effect between ultrasound dual frequency, temperature and time of purified polysaccharide were statistically significant. Therefore, the effect of ultrasound frequency, temperature and time was concluded to have had an effect on the extraction yield of purified polysaccharide.

Verification of predicted value of the models

The optimal conditions for the ultrasonic extraction were predicted at 34.02 °C, 20&60 KHz dual frequency, and time, 22.62 mins) for purified polysaccharides. The application of ultrasound to purified polysaccharide extraction was repeated at near optimum conditions by maintaining the predicted dual frequency (20 & 60 KHz) and modifying temperatures from 34.02 °C to 35 °C and time from 22.62 mins to 25 mins. In summary (Table 4), purified polysaccharide under the optimal predicted conditions and actual experimental showed close values. Also, an experiment conducted to reveal level of extraction of purified polysaccharide with ultrasound understated optimum conditions and without ultrasound (Fig. 5) confirmed the model to be the choicest.

Preliminary characterization of polysaccharides

Total carbohydrate, protein, phenolic and salt content

The chemical composition of SL-D_{20}P and SL-D_{30}P including total carbohydrate, protein and polyphenol content (Table 5) showed no much difference in values between the two purified samples. This showed that the dialysis process had no effect on the carbohydrate, protein and polyphenolic content.

Partially purified polysaccharides solution after 1 h application of DF-UAD was further kept in dialyzate for 5 h without ultrasound. The sample, SL-D_{20}P, had the dialyzate replaced every 20 mins within the 1 h of exposure to ultrasonic waves. It demonstrated a change in weight that ranged from 73 to 100%. The second sample, SL-D_{30}P, had the dialyzate replaced every 30 mins within 1 h of exposure to ultrasonic waves. It demonstrated a change in weight that ranged from 50 to 106%. The control sample was dialyzed without DF-UA and showed a change of weight that ranged from 42 to 78%. This implies SL-D_{30}P after dialysis process obtained a much less salt concentration (Table 6) due to greater salt replacement by dialyzate. This is in agreement with scientific reports that show that continuous cavitation occurs at the surface of filters used for filtration. Such cavitation prevents blockages of filters allowing for movements of small particles.[35]

Table 4. Predicted and actual experimental values of *Sorghum bicolor* leaves polysaccharide (%) extracted under modified optimal extraction conditions.

	Extraction Variables			
Type	X_1 (°C)	X_2 (KHz)	X_3 (mins)	Polysaccharide (%)
Optimum (Predicted)	34.02	20&60	29.62	16.11
Modified Optimum (Experimental)	35	20&60	30	16.02 ± 0.04

Table 5. Preliminary characterization of SL – D_{20}P and SL- D_{30}P.

Composition	SL – D_{20}P	SL – D_{30}P
Carbohydrate (%)	36.53 ± 0.05	36.12 ± 0.07
Protein (%)	0.30 ± 0.06	0.032 ± 0.04
Polyphenol (%)	22.23 ± 0.12	20.22 ± 0.08

Monosaccharide composition

The Fig. 6 (i) and (ii) showed that, the monosaccharide D-glucose was easily noticeable in SL-D_{20}P (19.19%) and SL-D_{30}P (9.61%) having used retention time and content for all six monosaccharides authentic standards (Fig. 6(a)). Also found in little amount was L-Arabinose, in SL-D_{20}P (5.39%) and (SL-D_{30}P) (3.83%). D-xylose and D-mannose were not detected in both samples.

Whiles SL-D_{20}P did not show any peak for galactose, it recorded a much higher galacturonic acid (75.42%). On the other hand, SL-D_{30}P recorded 22.70% galactose and a total amount of 63.85% galacturonic acid. This implies that DF-UAD under continuous mode and replacement of dialyzate every 20 mins for 1 h as part of a 6 h dialysis process caused the total oxidation of galactose to galacturonic acid. The effect of oxidation occurring under continuous mode of DF-UAD is similar to reported high lipid oxidation under continuous mode of ultrasound extraction.[36]

Spectral analysis

FT-IR spectra

The functional groups of extracted polysaccharides were studied using the FT-IR Spectroscopy (Fig. 7). It was revealed that SL-D_{20}P and SL-D_{30}P from *Sorghum*

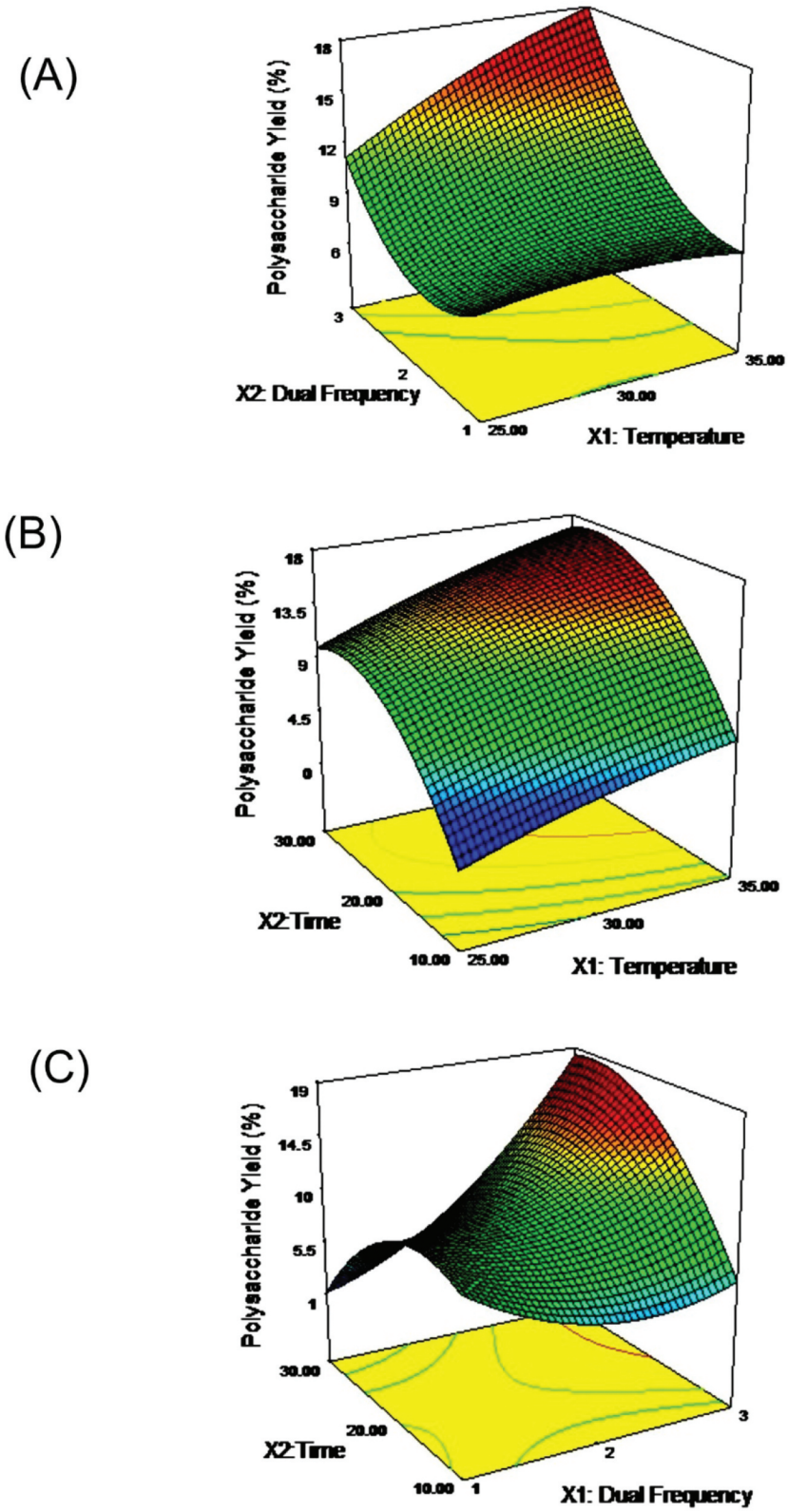

Figure 4. Response surface model plot showing the effects of independent variables on *Sorghum* Leaf sheath separated and purified polysaccharide yield: (**A)** temperature (°C) and dual frequency (KHz) **(B)** temperature (°C) and time (mins) **(C)** dual frequency (KHz) and time (mins). (Note: Dual frequency 40 & 60 = 1, Dual frequency 20 & 40 = 2 and Dual frequency 20 & 60 = 3).

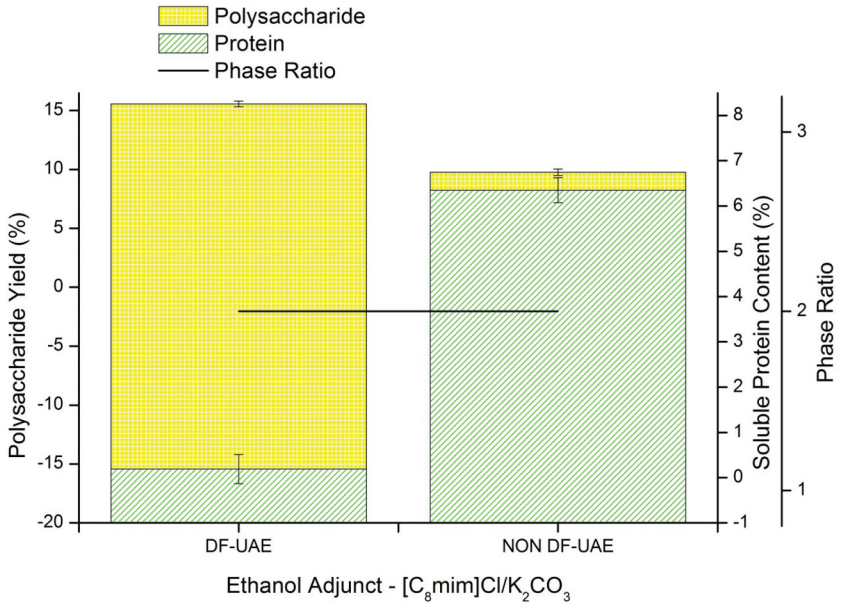

Figure 5. Effect of optimum dual ultrasound application on the extraction yield of simultaneously separated and purified polysaccharides and soluble proteins extracted into the bottom phase of the ethanol adjunct (40% v/v) ionic liquid aqueous two phase system, [C_8mim]Cl/K_2CO_3.

bicolor leaf sheath had similar peaks. Easily noticeable and usually associated with polysaccharides was the hydroxyl stretching vibration[37] by the bands at 3291 $cm^{-1}$and the stretching asymmetric vibration of C-H[37] and then also the stretching symmetric vibration of C-H[38] at the bands ranging from 2852 cm^{-1} – 2929 cm^{-1}. Furthermore, bands ranging 1,166 cm^{-1} – 1,200 cm^{-1} and 1004 cm^{-1} proposed peak related to C-C stretching vibration and C-O stretching vibration, respectively.

Ultraviolet spectra

The UV spectra of both SL-D_{20}P and SL-D_{30}P recorded no absorbance at 260 and 280 nm that depicted the absence of nucleic acid and protein after separation and purification process (Fig. 8). This proved a very successful deproteinization, combining DF-UAE and EA-ILATPS. The result was in agreement with the records on total protein (Table 5) of SL-D_{20}P and SL-D_{30}P.

Table 6. Effect of dual frequency ultrasound on liquid membrane dialysis of polysaccharides in salt-rich phase of ionic liquid aqueous two phase system, [C_8mim]Cl/K_2CO_3.

Time (Hours)	Δw (SL-D_{20}P)	Δw (SL-D_{30}P)	Δw (Without DF-UAD)
1	73.98	50.00	42.65
2	89.74	75.43	60.13
3	96.83	92.82	71.40
4	99.79	104.8	76.54
5	100.42	106.29	79.65
6	100.03	106.65	78.12

**DF-UAD = Dual frequency-ultrasound assisted dialysis*

Structural analysis

Polysaccharide conformation

The β-1, 3-linked glucose units of sorghum leaf sheath reported in literature was evident in the strong hypsochromic shift of SL-D_{20}P, moving from the maximum absorption to a shorter wavelength after the transition from triple-helix conformation in the congo red polysaccharide solution. On the other hand, after the separation, purification and dialysis process, SL-D_{30}P, also maintained its helical structure demonstrating a bathochromic shift, moving from its maximum absorption to a longer wavelength close to that of the negative control (Fig. 9).

Morphological analysis (SEM)

The DF-UA separated and purified polysaccharide SL-D_{20}P presented a transition-like structure. Basically, a combination of porous network-like and aggregated-like morphological structures was observed. It is worth noting that in our previous work,[2] replacement of dialyzate every 10 mins within a 1 h DF-UAD as part of 6 h dialysis process presented a porous network-like morphology. The sample SL-D_{30}P on the other hand, presented the absence of any porous network-like structures but large aggregated structures (Fig. 10). Large aggregated-like structures observed with SL-D_{30}P agreed with the notable large particle size recorded when dissolved in solution under room temperature (section 3.7.4) and further confirmation from records on it molecular weight

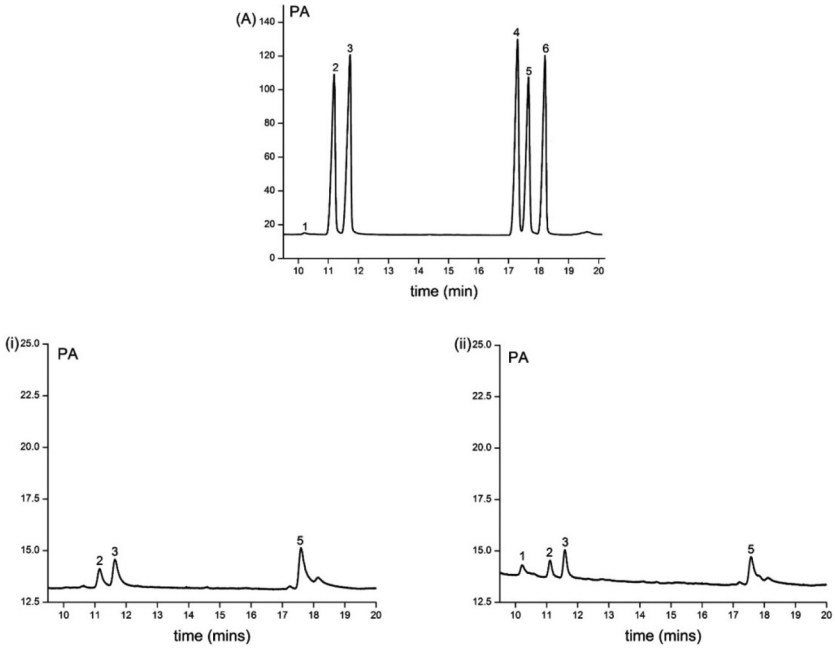

Figure 6. GC spectrum of monosaccharide composition of (A) monosaccharide reference, (i) SL-D_{20}P and (ii) SL-D_{30}P. The number 1 = D-galactose, 2 = L-arabinose, 3 = D-glucose, 4 = D-xylose, 5 = D-galacturonic acid, 6 = D-mannose.

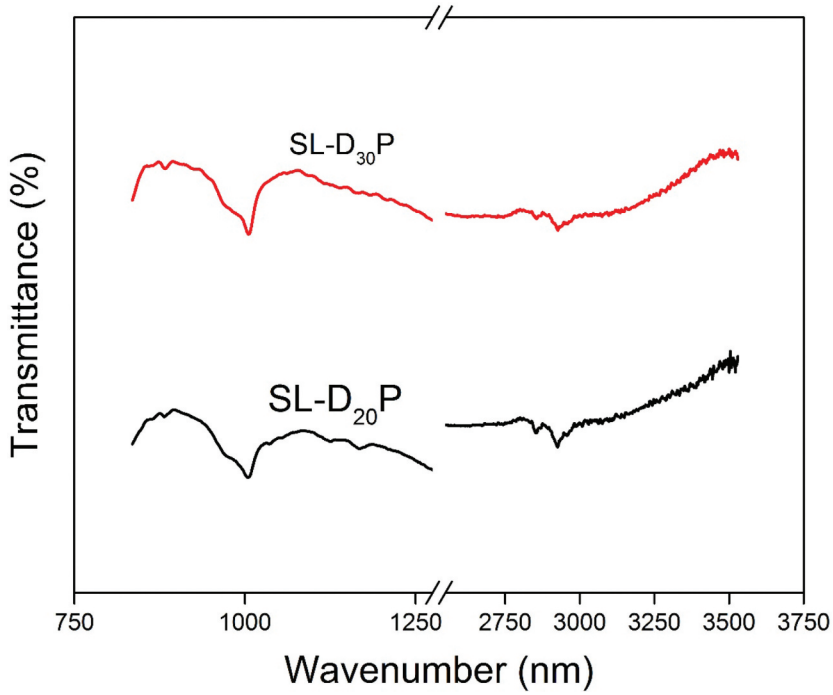

Figure 7. The FT-IR spectra of SL-D_{20}P and SL-D_{30}P polysaccharides.

which was beyond the maximum range of weight measurable using three columns in this work (section 2.10.3).

Molecular weight (HPSEC)

A molecular weight of (1,113,000 g/mol) was recorded for SL-D_{20}P after extraction and purification process (Table 7). Meanwhile, SL-D_{30}P demonstrated a molecular weight above working range of columns used during our experiments. Thus, prepared sample was too large to get trapped in the stationary phase. This is in agreement with the observed aggregated morphological structure (Fig. 10) and aggregated particle size when dissolved in water under room temperature (Fig. 11).

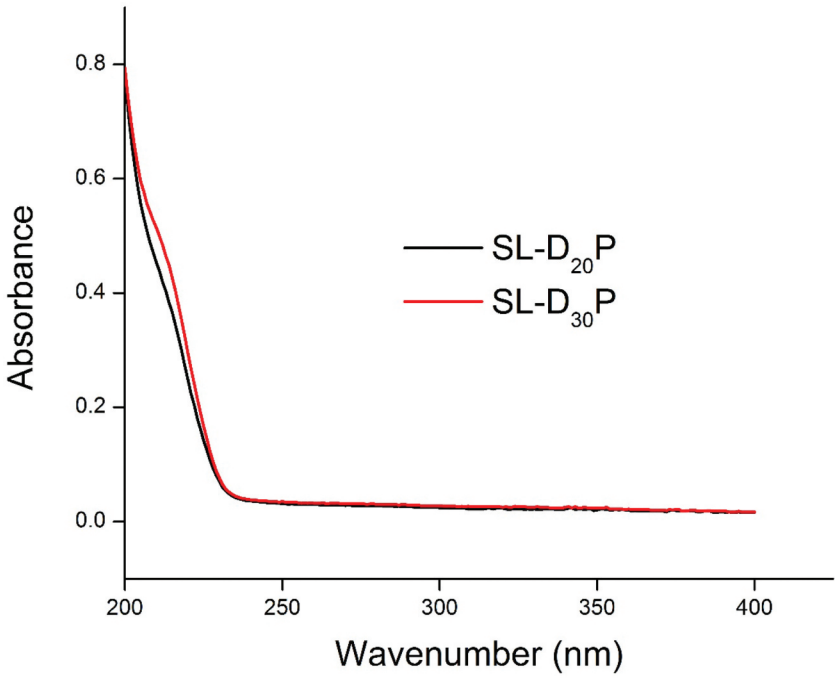

Figure 8. The UV-vis spectra of crude and IL-ATPS purified polysaccharide.

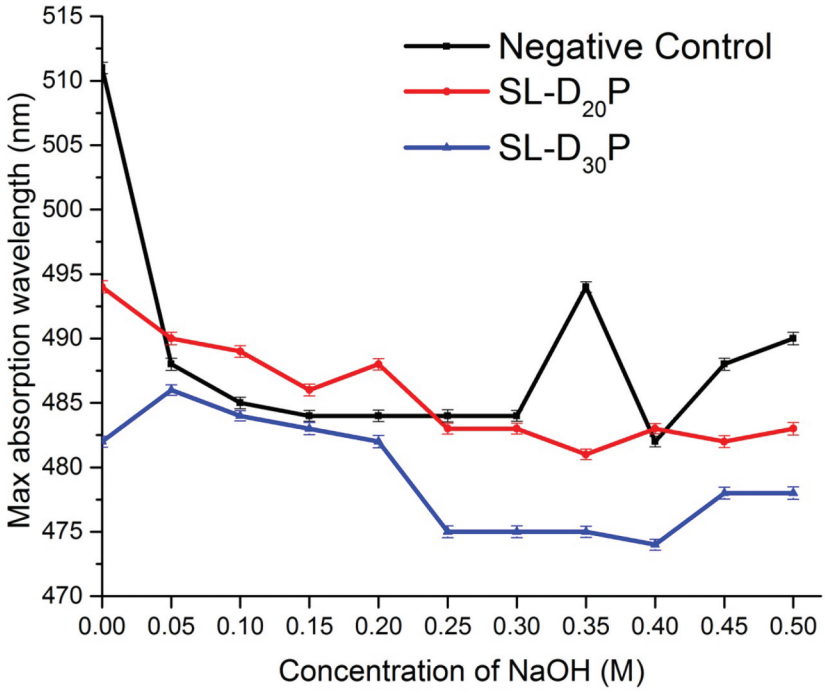

Figure 9. Helix-coil transition analysis of SL-D_{20}P and SL-D_{30}P.

Particle size (DLS)

The number particle size distribution of purified polysaccharides, SL-D_{20}P and SL-D_{30}P, in aqueous solutions was illustrated on (Fig. 11). When dispersed in water, particle size distribution with diameter for the former ranged (262.58 nm to 1,037.40 nm) and the latter (3,766.58 nm to 22,599.95 nm) with main peaks diameter at (521.93 nm and 9,226.30 nm), respectively. Having held the aqueous solution of SL-D_{20}P under a temperature of 70 °C for 1.5 h increment in particle size distribution was observed in the recorded area from (328.85 nm to 1,316.00 nm) and main peak (657.85 nm). Thus, hydrophobic forces in SL-D_{20}P after heat exposure rather intensified its aggregation.

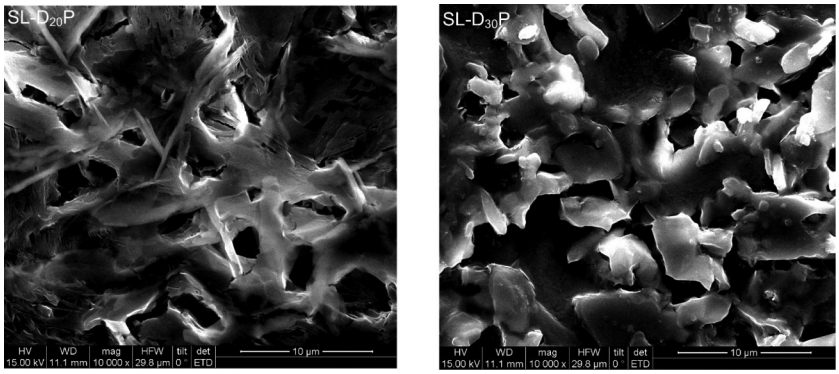

Figure 10. SEM of SL-D_{20}P and b) SL-D_{30}P.

Table 7. Molecular weight of polysaccharide (SL-D_{20}P) from *Sorghum bicolor* leaf sheath.

	Molecular weight (g/mol)				
Samples	Mn	Mp	Mw	Mz	Mw/Mn
SL-D_{20}P	1,090,000	965,000	1,113,000	1,143,000	1.021

This agrees with literature,[39] that most food polysaccharides can undergo heat-induced molecular aggregation based on supported conformational changes in their structure. On the other hand, SL-D_{30}P after heat exposure recorded a reduction in particle size distribution that ranged (258.03 nm to 946.65 nm) with a peak diameter at (494.23 nm). This confirms the irreversible effect of heat on the detachment of notably large aggregate of the polysaccharide SL-D_{30}P in water.

Rheological properties

The storage modulus (G′(of SL-D_{20}P and SL-D_{30}P demonstrated strong elasticity, with a consistent increase in frequency (1 to 10 Hz) (Fig. 12(a)). High molecular weight has been found to lead to easy overlap of molecules which causes easy formation of junction zones.[40] The loss modulus (G″) of SL-D_{30}P therefore demonstrated a faster junction zone formation due to the above working range molecular weight established under section 3.5.3 (Fig. 12(b)). SL-D_{30}P recorded slightly higher G″ values, making it slightly viscous. However, D_{20}P and SL-D_{30}P showed dominant elastic portion since tan δ was (< 1) under frequency (< 1 Hz) (Fig. 12(c)). The viscosity of both D_{20}P and SL-D_{30}P depicted a near – Newtonian flow behaviour, with constant records throughout the shear rate experiment (Fig. 12(d)).

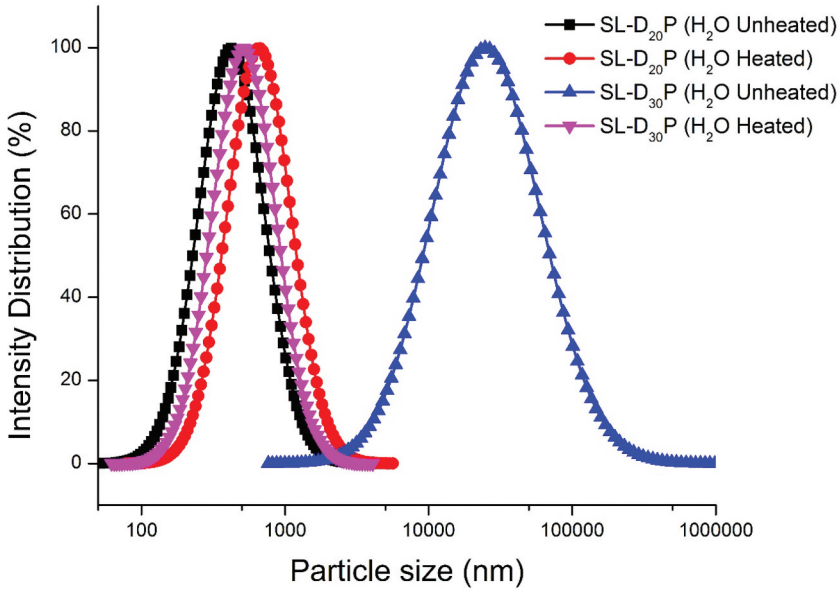

Figure 11. Particle size distribution of polysaccharides SL-D_{20}P and SL-D_{30}P in aqueous solution with or without heat.

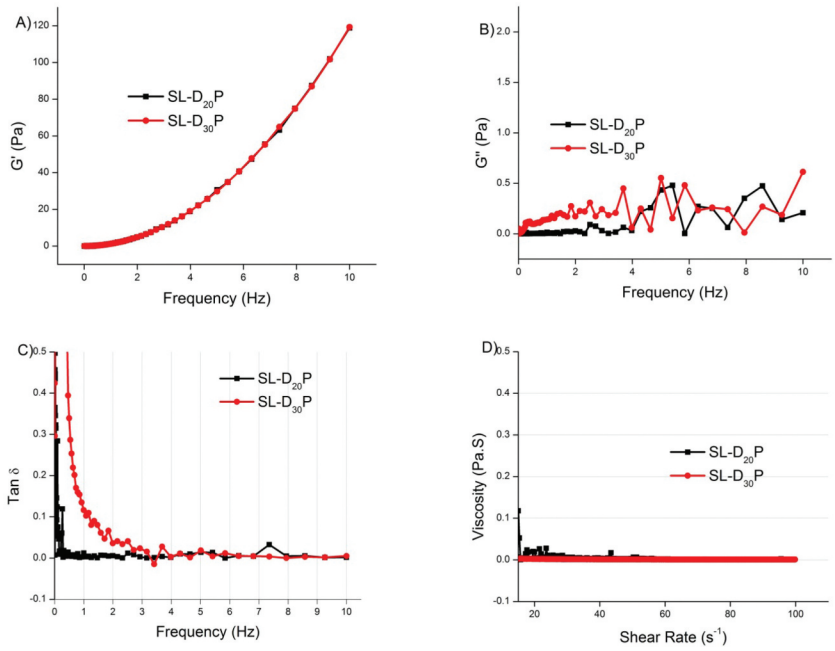

Figure 12. The storage modulus G′ A), loss modulus G′′ B), loss tangent tan δ dynamic frequency sweep test C) and D) steady shear flow curves of SL-D_{20}P and SL-D_{30}P polysaccharides.

Antioxidant activity

Scavenging effect on hydroxyl radical

Ascorbic acid, SL-D_{20}P and SL-D_{30}P hydroxyl radical scavenging activities have been displayed in (Fig. 13(a)) within a concentration range of 5–30 mg/ml. The samples SL-D_{20}P and SL-D_{30}P presented similar scavenging rate that ranged (56% – 67%). The positive control, ascorbic acid, however, had 80% scavenging rate. Meanwhile IC_{50} for ascorbic acid, SL-D_{20}P and SL-D_{30}P were 5 mg/ml, 8 mg/ml and 10 mg/ml respectively. This result has close relationship with total phenolic content recorded (Table 5) for the two extracted polysaccharide samples with SL-D_{30}P being slightly lower in value. Furthermore, polysaccharides with lower molecular weight have been found to give rise to higher hydroxyl scavenging activity.[41] This agrees with the determined molecular weight of the two samples.

Scavenging effect on ABTS radical

Correspondingly, Fig. 13(b), displays the ABTS radical scavenging activity of Ascorbic acid, SL-D_{20}P and SL-D_{30}P at different concentrations (5–30 mg/ml). Both extracted polysaccharide samples demonstrated a 100% scavenging rate for all experimental concentration whiles the ascorbic acid had very close range with negligible difference in scavenging rate of 99.75–100%. All three samples had an IC_{50} value of 5 mg/ml IC_{50}.

Conclusion

Simultaneously separated and purified polysaccharide with the aid of ethanol surfactant in an ionic liquid aqueous two phase system yielded a very remarkable yield of 16% under dual frequency ultrasound treatment. Though frequency of dialyzate replacement was varied

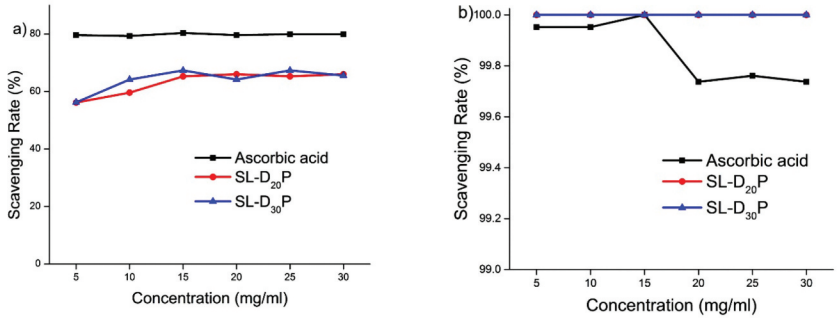

Figure 13. Scavenging effects of ascorbic acid, SL-D_{20}P and SL-D_{30}P polysaccharide on: (a) Hydroxyl radical and (b) ABTS radical.

under dual frequency ultrasound in the two working samples, total carbohydrate and proteins showed no much difference in values. Nevertheless, less frequent replacement of dialyzate aided in higher salt replacement (desalination). D-glucose was the predominant monosaccharide component in all samples but D-galactose was completely oxidized in SL-D_{20}P. The helical structure of *Sorghum bicolor* leaf sheath was intact after separation, purification and dialysis under dual frequency ultrasound. Morphological transition was displayed, from partly aggregate-like and partly porous network-like sample (SL-D_{20}P) to a fully aggregate-like sample (SL-D_{30}P). Whiles SL-D_{20}P sample aggregated after heat application in a solution, SL-D_{30}P aggregated nature was hydrolyzed after heat exposure. Both samples demonstrated elastic dominance and excellent ABTS radical scavenging abilities. These displayed characteristics of extracted polysaccharides can be fully utilized in various product developments in the food and pharmaceutical industry.

Funding

The authors are grateful for the support provided by the National Natural Science Foundation of China (21676125), the National Key Research and Development Program of China (2017YFD0400903-01, 2016YFD0400705-04), the Policy Guidance Program (Research Cooperation) of Jiangsu (BY2016072-03), the Social Development Program (General Project) of Jiangsu (BE2016779), and the Special Fund of Jiangsu Province for the Transformation of Scientific and Technological Achievements (BA2016169).

ORCID

Otu Phyllis Naa Yarley http://orcid.org/0000-0001-6042-7952
Cunshan Zhou http://orcid.org/0000-0001-9119-3941

References

[1] Tan, Z.-J.; Li, -F.-F.; Xu, X.-L.; Xing, J.-M. Simultaneous Extraction and Purification of Aloe Polysaccharides and Proteins Using Ionic Liquid Based Aqueous Two-phase System Coupled with Dialysis Membrane. *Desalination* 2012, 286, 389–393. DOI: 10.1016/j.desal.2011.11.053.

[2] Otu, P. N. Y.; Haonan, J.; Cunshan, Z.; Hongpeng, Y. Sorghum Bicolor L. Leaf Sheath Polysaccharides: Dual Frequency Ultrasound-assisted Extraction and Desalination. *Ind. Crops Prod.* 2018, 126, 368–379. DOI: 10.1016/j.indcrop.2018.10.032.

[3] Rosen, M. J.; Kunjappu, J. T. *Surfactants and Interfacial Phenomena*; John Wiley & Sons: Hoboken, New Jersey, 2012.

[4] Durkee, J. *Management of Industrial Cleaning Technology and Processes*; Elsevier: Amsterdam, The Netherlands, 2006.

[5] Somasundaran, P.; Lee, H.; Shchukin, E.; Wang, J. Cohesive Force Apparatus for Interactions between Particles in Surfactant and Polymer Solutions. *Colloids Surf. A* 2005, 266(1–3), 32–37. DOI: 10.1016/j.colsurfa.2005.05.073.

[6] Lonare, A. A.; Patel, S. R. Antisolvent Crystallization of Poorly Water Soluble Drugs. *Int. J. Chem. Eng. Appl.* 2013, 4(5), 337. DOI: 10.7763/IJCEA.2013.V4.321.

[7] Khatua, S.; Paul, S.; Acharya, K. Mushroom as the Potential Source of New Generation of Antioxidant: A Review. *Res. J. Pharm. Technol.* 2013, 6(5), 3.

[8] Lo, -T. C.-T.; Chang, C. A.; Chiu, K.-H.; Tsay, P.-K.; Jen, J.-F. Correlation Evaluation of Antioxidant Properties on the Monosaccharide Components and Glycosyl Linkages of Polysaccharide with Different Measuring Methods. *Carbohydr. Polym.* 2011, 86(1), 320–327. DOI: 10.1016/j.carbpol.2011.04.056.

[9] Kozarski, M.; Klaus, A.; Nikšić, M.; Vrvić, M. M.; Todorović, N.; Jakovljević, D.; Van Griensven, L. J. Antioxidative Activities and Chemical Characterization of Polysaccharide Extracts from the Widely Used Mushrooms Ganoderma Applanatum, Ganoderma Lucidum, Lentinus Edodes and Trametes Versicolor. *J. Food Compost. Anal.* 2012, 26(1–2), 144–153. DOI: 10.1016/j.jfca.2012.02.004.

[10] Park, I. Y.; Cho, J. H.; Kim, K. S.; Kim, Y.-B.; Kim, M. S.; Kim, S. C. Helix Stability Confers Salt Resistance upon Helical Antimicrobial Peptides. *J. Biol. Chem.* 2004, 279 (14), 13896–13901. DOI: 10.1074/jbc.M311418200.

[11] Dykes, L.; Rooney, L. W. Sorghum and Millet Phenols and Antioxidants. *J. Cereal Sci.* 2006, 44(3), 236–251. DOI: 10.1016/j.jcs.2006.06.007.

[12] Devi, P. S.; Kumar, M. S.; Das, S. M. Evaluation of Antiproliferative Activity of Red Sorghum Bran Anthocyanin on a Human Breast Cancer Cell Line (Mcf-7). *Int. J. Breast Cancer* 2011, 2011, 1–6. DOI: 10.4061/2011/891481.

[13] Lietti, A.; Cristoni, A.; Picci, M. Studies on Vaccinium Myrtillus Anthocyanosides. I. Vasoprotective and Antiinflammatory Activity. *Arzneimittel-Forschung* 1976, 26(5), 829–832.

[14] Tsuda, T.; Horio, F.; Osawa, T. The Role of Anthocyanins as an Antioxidant under Oxidative Stress in Rats. *Biofactors* 2000, 13(1-4), 133–139. DOI: 10.1002/biof.5520130122.

[15] Moholkar, V. S. Mechanistic Optimization of a Dual Frequency Sonochemical Reactor. *Chem. Eng. Sci.* 2009, 64(24), 5255–5267. DOI: 10.1016/j.ces.2009.08.037.

[16] Jiang, Y.; Xia, H.; Yu, J.; Guo, C.; Liu, H. Hydrophobic Ionic Liquids-assisted Polymer Recovery during Penicillin Extraction in Aqueous Two-phase System. *Chem. Eng. J.* 2009, 147(1), 22–26. DOI: 10.1016/j.cej.2008.11.012.

[17] Neves, C. M.; Ventura, S. P.; Freire, M. G.; Marrucho, I. M.; Coutinho, J. A. Evaluation of Cation Influence on the Formation and Extraction Capability of Ionic-liquid-based Aqueous Biphasic Systems. *J. Phys. Chem. B* 2009, 113(15), 5194–5199. DOI: 10.1021/jp900293v.

[18] Merchuk, J. C.; Andrews, B. A.; Asenjo, J. A. Aqueous Two-phase Systems for Protein Separation: Studies on Phase Inversion. *J. Chromatogr. B Biomed. Sci. Appl.* 1998, 711(1), 285–293. DOI: 10.1016/S0378-4347(97)00594-X.

[19] Zhang, X.; Ban, Q.; Wang, X.; Wang, Z. Green and Efficient PEG-based Ultrasonic-assisted Extraction of Polysaccharides from Tree Peony Pods and the Evaluation of Their Antioxidant Activity in Vitro. *Biomed Res. Int.* 2018, 2018, 1–7. DOI: 10.1155/2018/2121385.

[20] DuBois, M.; Gilles, K. A.; Hamilton, J. K.; Rebers, P. A.; Smith, F. Colorimetric Method for Determination of Sugars and Related Substances. *Anal. Chem.* 1956, 28 (3), 350–356. DOI: 10.1021/ac60111a017.

[21] Bradford, M. M. A Rapid and Sensitive Method for the Quantitation of Microgram Quantities of Protein Utilizing the Principle of Protein-dye Binding. *Anal. Biochem.* 1976, 72(1–2), 248–254.

[22] Kumar, K. S.; Ganesan, K.; Rao, P. S. Antioxidant Potential of Solvent Extracts of Kappaphycus Alvarezii (Doty) Doty–An Edible Seaweed. *Food Chem.* 2008, 107 (1), 289–295. DOI: 10.1016/j.foodchem.2007.08.016.

[23] Wang, J.; Lian, P.; Yu, Q.; Wei, J.; Kang, W.-Y. Purification, Characterization and Procoagulant Activity of Polysaccharides from Angelica Dahurice Roots. *Chem. Cent. J.* 2017, 11(1), 17. DOI: 10.1186/s13065-017-0243-y.

[24] Qiu, T.; Ma, X.; Ye, M.; Yuan, R.; Wu, Y. Purification, Structure, Lipid Lowering and Liver Protecting Effects of Polysaccharide from Lachnum YM281. *Carbohydr. Polym.* 2013, 98(1), 922–930. DOI: 10.1016/j.carbpol.2013.07.014.

[25] Ren, L.; Edwards, P. J.; Perera, C. O.; Hemar, Y. Structural Features of a Novel Polysaccharide Isolated from a New Zealand Maori Mushroom Iliodiction Cibarium. *Carbohydr. Res.* 2015, 406, 19–26. DOI: 10.1016/j.carres.2014.12.011.

[26] Jen, J.-F.; Leu, M.-F.; Yang, T. C. Determination of Hydroxyl Radicals in an Advanced Oxidation Process with Salicylic Acid Trapping and Liquid Chromatography. *J. Chromatogr. A* 1998, 796(2), 283–288. DOI: 10.1016/S0021-9673(97)01019-4.

[27] Zhou, H.-C.; Lin, Y.-M.; Li, -Y.-Y.; Li, M.; Wei, S.-D.; Chai, W.-M.; Tam, N. F.-Y. Antioxidant Properties of Polymeric Proanthocyanidins from Fruit Stones and Pericarps of Litchi Chinensis Sonn. *Food Res. Int.* 2011, 44(2), 613–620. DOI: 10.1016/j.foodres.2010.12.016.

[28] Pei, Y.; Wang, J.; Liu, L.; Wu, K.; Zhao, Y. Liquid–Liquid Equilibria of Aqueous Biphasic Systems Containing Selected Imidazolium Ionic Liquids and Salts. *J. Chem. Eng. Data* 2007, 52(5), 2026–2031. DOI: 10.1021/je700315u.

[29] Dutta, R.; Kundu, S.; Sarkar, N. Ionic Liquid-induced Aggregate Formation and Their Applications. *Biophys. Rev.* 2018, 10(3), 861–871. DOI: 10.1007/s12551-018-0408-5.

[30] Yan, J.; Joshee, N.; Liu, S. Utilization of Hardwood in Biorefinery: A Kinetic Interpretation of Pilot-scale Hot-water Pretreatment of Paulownia Elongata Woodchips. *J. Biobased Mater. Bioenergy* 2016, 10(5), 339–348. DOI: 10.1166/jbmb.2016.1609.

[31] Liu, S. Woody Biomass: Niche Position as a Source of Sustainable Renewable Chemicals and Energy and Kinetics of Hot-water Extraction/hydrolysis. *Biotechnol. Adv.* 2010, 28(5), 563–582. DOI: 10.1016/j.biotechadv.2010.05.006.

[32] Xie, X.; Wang, Y.; Han, J.; Yan, Y. Extraction Mechanism of Sulfamethoxazole in Water Samples Using Aqueous Two-phase Systems of Poly (Propylene Glycol) and Salt. *Anal. Chim. Acta* 2011, 687(1), 61–66. DOI: 10.1016/j.aca.2010.12.012.

[33] He, P. Z.; Xia, R. M.; Duan, S. M.; Shou, W. D.; Qian, D. C. The Affection on the Tissue Lesions of Difference Frequency in Dual-frequency High-intensity Focused Ultrasound (HIFU). *Ultrason. Sonochem.* 2006, 13(4), 339–344. DOI: 10.1016/j.ultsonch.2005.05.008.

[34] Yong-Guang, B.; Ding-Long, Y.; Yu-min, L.; Min-xia, H. Study on Ultrasonic-assisted Extraction of Polysaccharide of Atractylis Macroceohala Koidz of Experiment. *Energy Procedia* 2012, 17, 1778–1785. DOI: 10.1016/j.egypro.2012.02.311.

[35] Feng, H.; Barbosa-Cánovas, G. V.; Weiss, J. *Ultrasound Technologies for Food and Bioprocessing*; Springer: New York, 2011.

[36] Gulzar, S.; Benjakul, S. Ultrasound Waves Increase the Yield and Carotenoid Content of Lipid Extracted from Cephalothorax of Pacific White Shrimp (Litopenaeus Vannamei). *Eur. J. Lipid Sci. Technol.* 2018, 120(5), 1700495. DOI: 10.1002/ejlt.201700495.

[37] Geddes, C. D.; Lakowicz, J. R. *Glucose Sensing*; Springer Science & Business Media: United States of America, 2007.

[38] Dopico, A. M.; Tigyi, G. J. *A Glance at the Structural and Functional Diversity of Membrane Lipids Methods in Membrane Lipids*; Springer: United States of America, 2007.

[39] Telis, V. R. N. *Biopolymer Engineering in Food Processing*; CRC Press: Boca Raton, FL, U.S.A., 2012.

[40] Freitas, F.; Alves, V. D.; Carvalheira, M.; Costa, N.; Oliveira, R.; Reis, M. A. Emulsifying Behaviour and Rheological Properties of the Extracellular Polysaccharide Produced by Pseudomonas Oleovorans Grown on Glycerol Byproduct. *Carbohydr. Polym.* 2009, 78(3), 549–556. DOI: 10.1016/j.carbpol.2009.05.016.

[41] Xie, J.-H.; Shen, M.-Y.; Xie, M.-Y.; Nie, S.-P.; Chen, Y.; Li, C.; Huang, D.-F.; Wang, Y.-X. Ultrasonic-assisted Extraction, Antimicrobial and Antioxidant Activities of Cyclocarya Paliurus (Batal.) Iljinskaja Polysaccharides. *Carbohydr. Polym.* 2012, 89(1), 177–184. DOI: 10.1016/j.carbpol.2012.02.068.